



Society of Petroleum Engineers

SPE-216776-MS

Use of Critical Point in Equation of State Modeling for Reservoir Fluids

K. S. Pedersen and P. L. Christensen, Kapexy Aps, Kgs. Lyngby, Denmark; J. A. Shaikh, Calsep FZ, LLC, Dubai, UAE

Copyright 2023, Society of Petroleum Engineers DOI [10.2118/216776-MS](https://doi.org/10.2118/216776-MS)

This paper was prepared for presentation at the ADIPEC held in Abu Dhabi, UAE, 2 – 5 October, 2023.

This paper was selected for presentation by an SPE program committee following review of information contained in an abstract submitted by the author(s). Contents of the paper have not been reviewed by the Society of Petroleum Engineers and are subject to correction by the author(s). The material does not necessarily reflect any position of the Society of Petroleum Engineers, its officers, or members. Electronic reproduction, distribution, or storage of any part of this paper without the written consent of the Society of Petroleum Engineers is prohibited. Permission to reproduce in print is restricted to an abstract of not more than 300 words; illustrations may not be copied. The abstract must contain conspicuous acknowledgment of SPE copyright.

Abstract

Several equations of state have been proposed as a supplement or a replacement for cubic equations, but cubic equations have remained an industry standard in the petroleum industry. Cubic equations are bound to correctly predict the critical point of each component in an oil or gas mixture. With a minor correction, the location of the critical point also determines the simulated gas and liquid properties of a pure component at other pressures and temperatures. Also, for multicomponent reservoir fluids, the location of the critical point exerts a large influence on the phase behavior of the fluid in the entire gas and liquid region. The paper presents procedures that, for both reservoir oils and gas condensates, allow a reliable equation of state model to be generated with a fluid composition and an experimental saturation point as the only experimental data. This is possible by using an estimated critical point as an artificial data point. For oils, the estimated critical point is for the entire reservoir fluid, while for gas condensates it is the critical point of the C₇₊ fraction, since not all gas condensates have a critical point. The method can also be used to quality check existing EoS models or as an additional constraint when developing an EoS model by regression to experimental PVT data. This is particularly useful for heavily lumped EoS models.

Introduction

The first cubic equation of state was proposed by van der Waals (vdW) [1], and relates P, V and T through two parameters, a and b that are unique functions of the critical temperature and pressure. The vdW equation thereby expresses that the phase behavior of a pure component in the entire gas and liquid region is determined by the location of the critical point. Today, the most used equations of state for petroleum reservoir fluids are the Soave-Redlich-Kwong (SRK) [2] and the Peng-Robinson (PR) [3] equations. These have retained the basic idea that the phase behavior of a pure component is determined by the location of the critical point but an acentric factor has been introduced to fine-tune the interaction between the molecules at temperatures deviating from the critical one. For a multicomponent system, the equation of state is also to simulate the phase amounts and compositions. That adds an extra dimension to equation of state modeling for reservoir fluids as compared to the case with a single component.

The top left plot of [Figure 1](#) shows the simulated phase envelope (dew and bubble point lines) of a gas condensate mixture. Also shown are iso-volume (quality) lines connecting pressures and temperatures with

equal gas and liquid volume fractions. The experimental saturation pressure at the reservoir temperature of 405 K is marked with a square and the simulated critical point with a dot. The top right plot in [Figure 1](#) shows a simulated phase envelope for the same fluid with the equation of state parameters tuned to give a simulated critical temperature that is 40 K higher than in the left-hand plot (300 K instead of 260 K) while still matching the experimental saturation pressure. All iso-volume lines are bound to meet at the critical point. The vertical lines showing the reservoir temperature intersect the iso-volume lines at different volume fractions in the two plots. This illustrates the importance of the location of the critical point. The two bottom plots in [Figure 1](#) show how much the difference in critical point impacts the liquid drop out (liquid volume% of saturation point volume) in a constant mass expansion (CME) experiment [4]. When the critical temperature for a gas condensate gets closer to the temperature at which a pressure depletion experiment is conducted (bottom right-hand plot), the liquid dropout curve gets steeper, and more liquid precipitates relative to the volume at the saturation pressure.

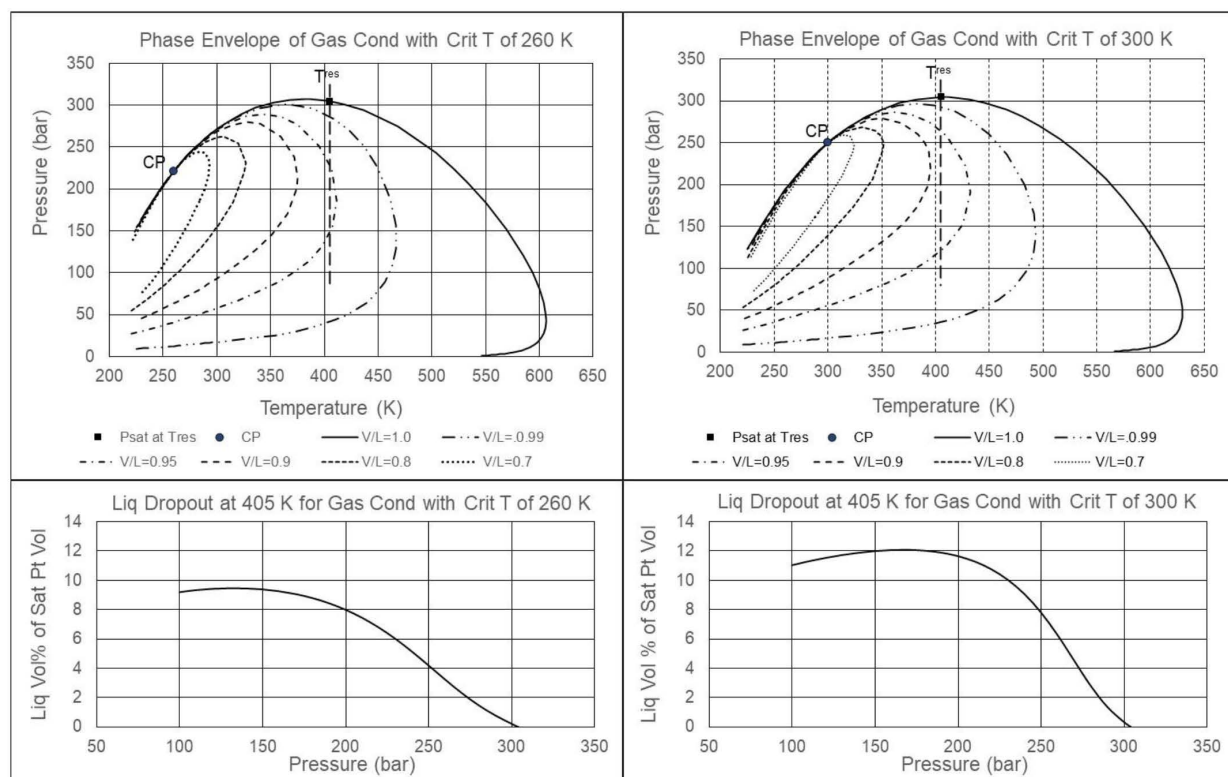


Figure 1—Simulated phase envelopes (upper plots) for a gas condensate with iso-volume (quality) lines. Two different EoS model descriptions have been used. The experimental saturation pressure of 304 bar at 405 K is matched with both models but the critical temperature deviates by 40 K. The bottom two plots show what the difference in critical temperature means for the simulated CME liquid dropout curves at the reservoir temperature.

Similar plots are shown for a volatile oil in [Figure 2](#). When the equation of state parameters are tuned up to give a simulated critical temperature of the fluid closer to the experimental CME temperature (right-hand plots), the fluid will behave more near-critical and the liquid dropout curve (which for an oil starts at 100% liquid) becomes steeper (higher liquid shrinkage).

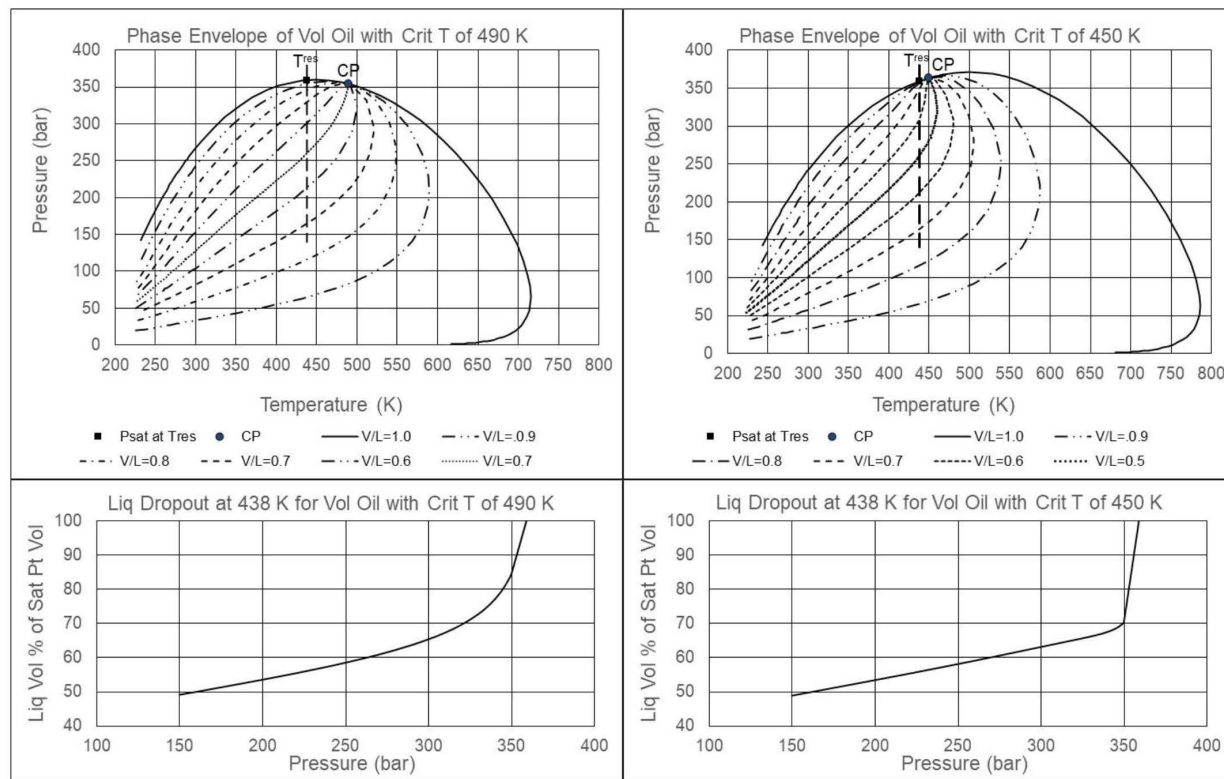


Figure 2—Simulated phase envelopes (upper plots) for a volatile oil with iso-volume (quality) lines. Two different EoS model descriptions have been used. The experimental saturation pressure of 368 bar at 438 K is matched with both models but the critical temperature deviates by 40 K. The bottom two plots show what the difference in critical temperature means for the simulated CME liquid dropout curves at the reservoir temperature.

These simulation results show that the location of the critical point for a reservoir fluid is of great importance for how the fluid behaves, not only at conditions close to the critical point, but also at pressures and temperatures far from the critical point. An equation of state model for a reservoir fluid will only be generally applicable if it predicts the correct critical point of the fluid.

Reservoir Fluid Characterization

Reservoir fluids can be divided into two component groups, defined components to C₆ and C₇₊ components. This distinction is practical because it is not possible to identify all the C₇₊ components. While the components, N₂, CO₂, H₂S and C₁-C₆, have well defined equation of state parameters (T_c, P_c, and acentric factor), the C₇₊ fraction must be split into pseudo-components whose equation of state parameters are found from correlations in measurable properties, often molecular weight and density. The T_c's of C₇₊ components increase with increasing molecular weight, while the P_c's decrease. The acentric factors have less influence on the phase behavior and the development of the acentric factors with molecular weight is less well defined, but it is established that the acentric factors increase to around C₅₀, after which a decrease can be seen as the concentration of aromatic components increases, which component group has lower acentric factors than paraffins, the dominant component group in lower carbon number fractions.

Experimental data [5,6] and chemical reaction theory [7,8] have shown a linear relationship between the logarithm of the mole fraction (z_i) of the ith C₇₊ fraction and its carbon number (C_n_i)

$$\ln(z_i) = A + B \times C_{n_i} \quad (1)$$

where A and B are constants. Assuming the following relation exists between molecular weight and carbon number

$$M_i = 14Cn_i - 4 \quad (2)$$

and that C_{80} is the heaviest carbon number fraction to be considered, A and B can be determined from the average molecular weight of the total C_{7+} fraction. This allows the mole fractions of all C_{7+} fractions to C_{80} to be determined regardless of whether the composition stops at C_{7+} , C_{20+} , C_{36+} , or another carbon number. Pedersen et al. [6,9] have proposed the below correlations to be used for C_{7+} carbon number fraction i:

$$T_{ci} = c_1\rho_i + c_2\ln(M_i) + c_3M_i + \frac{c_4}{M_i} \quad (3)$$

$$\ln(P_{ci}) = d_1 + d_2\rho_i^{d_5} + \frac{d_3}{M_i} + \frac{d_4}{M_i^2} \quad (4)$$

$$m_i = e_1 + e_2M_i + e_3\rho_i + e_3M_i^2 \quad (5)$$

where M_i is the molecular weight and ρ_i the density of the i^{th} fraction. For the SRK equation [2] the parameter m_i is related to the acentric factor (ω_i) through:

$$m_i = 0.480 + 1.574\omega_i - 0.176\omega_i^2 \quad (6)$$

while the PR equation uses the below expression for m_i

$$m_i = 0.37464 + 1.54226\omega_i - 0.26992\omega_i^2 \quad (7)$$

The coefficients in Equations (3) – (5) to be used with the SRK and PR equations are given in Table 1.

Table 1—Coefficients in Equations (3) - (5) [6,9] for use with the SRK [2] and PR [3] equations of state.

Coefficient/Sub-index	1	2	3	4	5
SRK					
c	1.6312×10^2	8.6052×10	4.3475×10^{-1}	-1.8774×10^3	
d	-1.3408×10^{-1}	2.5019	2.0846×10^2	-3.9872×10^3	1.0
e	7.4310×10^{-1}	4.8122×10^{-3}	9.6707×10^{-3}	-3.7184×10^{-6}	
PR					
c	7.34043×10	9.73562×10	6.18744×10^{-1}	-2.05932×10^3	
d	7.28462×10^{-2}	2.18811	1.63910×10^2	-4.04323×10^3	0.25
e	3.73765×10^{-1}	5.49269×10^{-3}	1.17934×10^{-2}	-4.93049×10^{-6}	

Figure 3 schematically shows how the T_c 's of P_c 's of the C_{7+} pseudo-components develop with molecular weight according to Equations (3) and (4). T_c increases with increasing molecular weight while P_c decreases. The higher the molecular weight of a C_{7+} pseudo-component, the more uncertain the T_c of P_c to be assigned to it. Christensen [10] has addressed this uncertainty by proposing a regression procedure that starts with the T_c and P_c curves obtained with Equations (3) and (4) and the coefficients in Table 1. Maintaining T_c and P_c of C_7 , the curves are rotated to obtain the equation of state model description providing the best possible match to the experimental PVT data. This rotation is sketched with dashed lines in Figure 3.

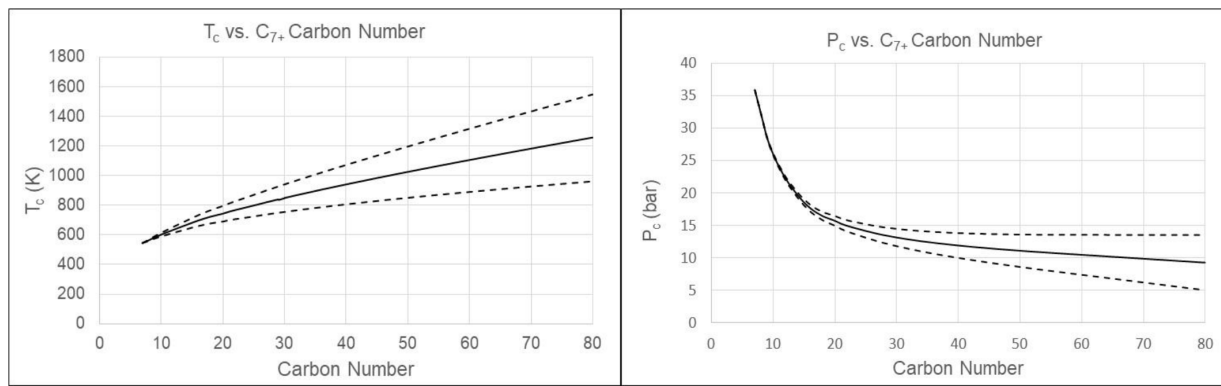


Figure 3—Regression technique [10] used to find the optimum T_c 's and P_c 's of the C_{7+} pseudo-components. The T_c and P_c curves found using Equations (3) and (4) with the coefficients in Table 1 (full drawn lines) are rotated around T_c and P_c of C_7 to give the freedom sketched with the dashed lines.

Critical Point of a Reservoir Fluid

The outlined characterization procedure presents one problem. An increase or a decrease of either the T_c 's or P_c 's of the heaviest pseudo-components may have approximately the same influence on the simulated saturation pressure and volumetric properties at the reservoir temperature. Further information is needed to balance the modifications of the T_c 's and P_c 's to also represent the phase behavior at other temperatures than that in the reservoir. Pedersen et al. [11] have proposed adding a constraint to the regression technique illustrated in Figure 3 by forcing an estimated critical point of the total mixture to be matched. The correlations below were proposed to estimate the critical point (T_{c_mix} , P_{c_mix}) of a reservoir fluid after removal of non-hydrocarbons for which at least 10 mol% of the hydrocarbons are C_{7+} components.

$$T_{c_mix} = a_1 + a_2 \times \ln\left(\frac{\text{Mole } C_{7+}}{\text{Mole } C_1 - C_6}\right) + a_3 \times \left(\frac{\text{Mole } C_{7+}}{\text{Mole } C_1 - C_6}\right)^{-1} \quad (8)$$

$$P_{c_mix} = a_4 \times \left(\frac{\text{Mole } C_{7+}}{\text{Mole } C_1 - C_6}\right)^{a_5} \quad (9)$$

For oil mixtures, the critical point was determined from data for swelling experiments that were continued until the saturation point changed from a bubble point to a dew point. A critical fluid composition exists between the last bubble point and the first dew point. The C_{7+} fraction is assigned an EoS model description that matches the critical point for the reservoir fluid with added gas. The same EoS model is subsequently used for the reservoir fluid without added gas, and the assumption is that the critical point simulated for this fluid is the correct one. The data material used to develop the above correlations also included near-critical fluids. That means fluids for which the critical point is close to the saturation pressure at the reservoir temperature. The values of the coefficients a_1-a_5 proposed by Pedersen et al. [11] for use with the SRK equation are shown in Table 2 together with coefficients for use with the PR equation estimated in this work using the same procedure.

Table 2—Coefficients in Equations (8) and (9) for use with the SRK [2] and PR [3] equations to estimate T_{c_mix} in K and P_{c_mix} in bar for a petroleum reservoir fluid after removal of non-hydrocarbons for which at least 10 mol% of the hydrocarbons are C_{7+} components.

Coefficient	SRK ^{*1}	PR
a_1	683.88	692.44
a_2	26.128	53.981
a_3	-34.061	-26.250
a_4	98.035	110.86

Coefficient	SRK ^{*1)}	PR
a ₅	-0.674	-0.611

*1)From [11]

Reservoir fluids for which at least 10 mol% of the hydrocarbons are C₇₊ compounds will either be oil mixtures or near critical fluids. That means the critical temperature will either be higher than or close to the reservoir temperature. The left-hand plot of Figure 4 shows simulated phase envelopes for three reservoir oil mixtures, a volatile oil, a black oil, and a heavy oil. The C₇₊ concentration increases in this order. The critical temperatures of these three oil compositions increase with increasing C₇₊ mol% in accordance with Equation (8), while the critical pressures in accordance with Equation (9) decrease with increasing C₇₊ mol%.

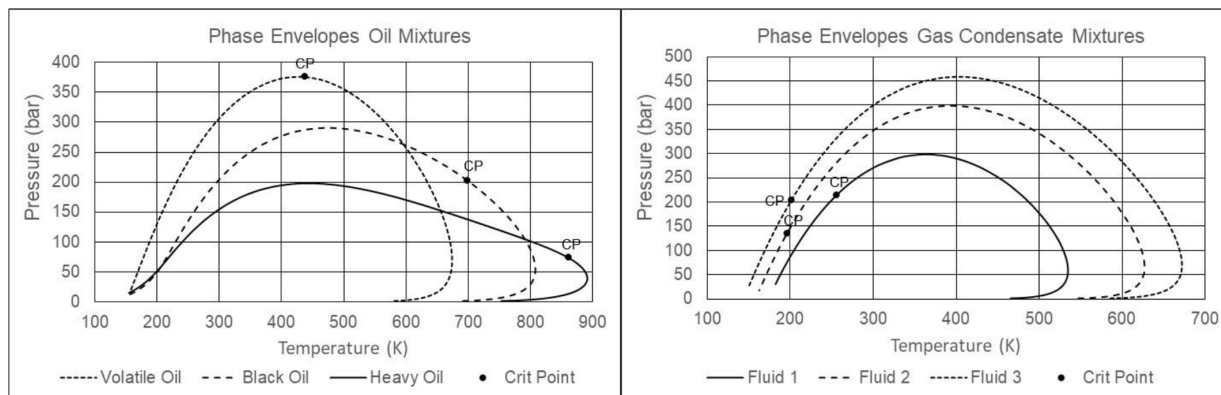


Figure 4—Simulated phase envelopes for a volatile oil, a black oil and a heavy oil (left-hand) and (right-hand) simulated phase envelopes for three gas condensate mixtures of the compositions in Table 3. The three gas condensates have C₇₊ mol%'s of 5.15, 6.58 and 7.51, respectively.

The right-hand plot of Figure 4 shows simulated phase envelopes for three gas condensate mixtures (Fluids 1–3 in Table 3) characterized for the SRK equation. To make the simulated phase envelopes comparable, the inorganic components (N₂, CO₂ and H₂S) have been removed. The total C₇₊ mol% in each fluid after removal of inorganics can be seen from Table 3 and is for all three fluids lower than the 10% validity limit for Equations (8) and (9). In contrast to what is seen for the oil mixtures, gas condensates do not show a clear trend in how the critical point develops with C₇₊ concentration.

Table 3—Four gas condensate reservoir fluid compositions. Simulated phase envelopes of Fluids 1–3 after removal of non-hydrocarbons are shown in Figure 4. The simulated phase envelope of Fluid 4 is shown in Figure 5. The last column shows the composition of the C₇₊ fraction of Fluid 4. Its estimated critical temperature and pressure are determined from Equations (10) and (11) using the SRK coefficients in Table 8.

Component	Fluid 1	Fluid 2	Fluid 3	Fluid 4	C ₇₊ Fraction of Fluid 4
	Mol%	Mol%	Mol%	Mol%	Mol%
N ₂	0.130	0.643	0.532	0.670	
CO ₂	2.990	3.531	3.304	2.410	
H ₂ S	0.810	0.000	0.000	0.000	
C ₁	74.370	70.767	72.985	84.480	
C ₂	7.950	8.940	7.680	4.590	
C ₃	3.740	5.050	4.099	2.520	
iC ₄	0.820	0.848	0.702	0.440	

Component	Fluid 1	Fluid 2	Fluid 3	Fluid 4	C ₇₊ Fraction of Fluid 4
	Mol%	Mol%	Mol%	Mol%	Mol%
nC ₄	1.690	1.679	1.421	0.890	
iC ₅	0.710	0.622	0.539	0.310	
nC ₅	0.820	0.788	0.669	0.380	
C ₆	1.000	0.828	0.849	0.410	
C ₇	1.000	1.059	1.330	0.550	18.966
C ₈	0.970	1.060	1.332	0.490	16.897
C ₉	0.760	0.790	0.780	0.410	14.138
C ₁₀₍₊₎	0.550	0.570	0.610	1.450	50.000
C ₁₁	0.380	0.379	0.421		
C ₁₂	0.280	0.370	0.330		
C ₁₃	0.220	0.319	0.420		
C ₁₄	0.170	0.270	0.240		
C ₁₅	0.140	0.230	0.300		
C ₁₆	0.110	0.190	0.169		
C ₁₇	0.080	0.170	0.210		
C ₁₈	0.060	0.130	0.150		
C ₁₉	0.050	0.130	0.150		
C ₂₀₊	0.180	0.637	0.778		
C ₇₊ Molecular Weight	141.0	164.7	167.9	145.1	145.1
C ₇₊ Density (g/cm ³)	0.7800	0.8125	0.8164	0.7949	0.7949
C ₇₊ mol% of total HC	5.15	6.58	7.51	2.99	—
Reservoir Temperature (T ^{res}) in K	406.2	423.7	416.2	403.2	—
Saturation Pressure (bar) at T ^{res}	304.0	381.0	447.8	365.8	—
Estimated Critical Temperature (K)					628.5
Estimated Critical Pressure (bar)					32.8

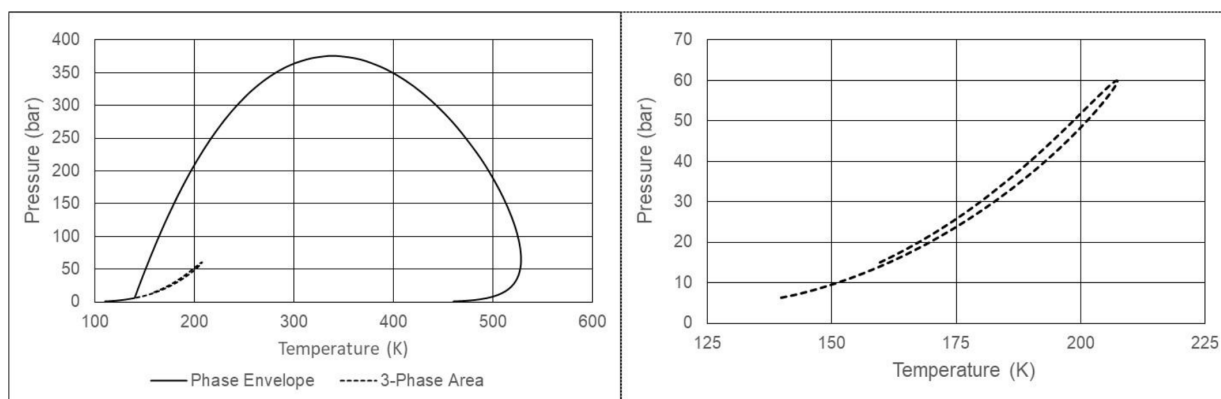


Figure 5—Simulated phase envelope for Fluid 4 in Table 3 (left-hand) and enlargement of 3-phase area (right-hand).

For gas condensates it is an additional challenge that not all gas condensates have a critical point. The left-hand plot of [Figure 5](#) shows the phase envelope of a light gas condensate (Fluid 4 in [Table 3](#)) characterized for the SRK equation. This gas condensate has a 3-phase area at low temperature and pressure, but no critical point. The right-hand plot of [Figure 5](#) shows an enlargement of the 3-phase area.

When a reservoir fluid has a critical point as is the case for the fluids for which phase envelopes are shown in [Figure 4](#), the portion of the phase envelope on the low-temperature side of the critical point is a bubble point line separating a liquid region outside the phase envelope from a 2-phase gas-liquid region inside the phase envelope. For Fluid 4 and other light gas condensates without a critical point, the low temperature branch of the phase envelope separates two liquid-like phases. At low pressure, a third phase forms as seen from [Figure 5](#). This is a gas phase rich in methane. Such reservoir fluid never reaches a state where two identical phases are in equilibrium, as is the case at a critical point.

Critical Point of C₇₊ Fraction

To overcome the challenges with gas condensate reservoir fluids, the C₇₊ fraction of a gas condensate (almost identical to the liquid from a flash of the gas condensate to standard conditions) will be considered a separate fluid. A fluid consisting of the C₇₊ fraction will have a critical point, which enables correlations to be developed to estimate this critical point. Once the C₇₊ fraction is correctly described, it is straightforward to add the defined components (N₂, CO₂, H₂S and C₁-C₆) to obtain an EoS model for the entire reservoir fluid, since the critical properties of the defined components are known. [Table 4](#) shows constant volume depletion (CVD) and constant mass expansion (CME) liquid dropout curves for Fluids 1-4 in [Table 3](#). Using the regression technique illustrated by the dashed lines in [Figure 3](#), C₇₊ equation of state parameters for use with the volume corrected SRK equation [2,12] were determined for Fluids 1-3 and shown in [Table 5](#). The literature equation of state parameters [13] listed in [Table 6](#) were used for the defined components. [Figure 6](#) shows experimental and simulated liquid dropout data.

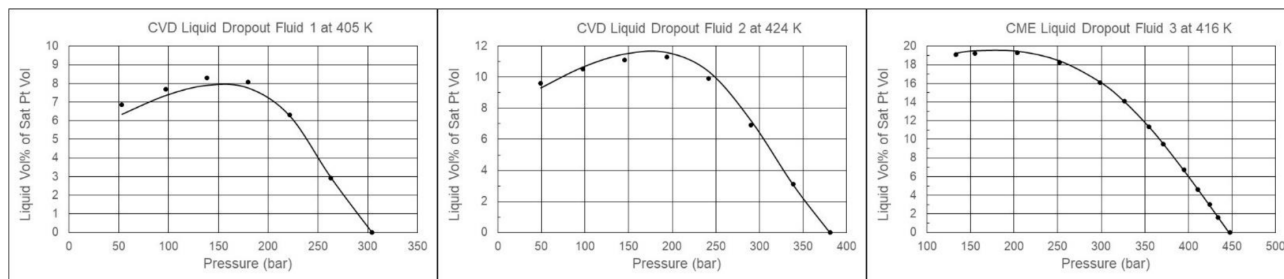


Figure 6—Experimental (●) and simulated (—) liquid dropout curves for Fluids 1-3 in [Table 3](#) with the C₇₊ fractions characterized as shown in [Table 5](#) and using the equation of state parameters in [Table 6](#) for the defined components. The volume corrected SRK equation [2,12] was used in the simulations.

Table 4—Experimental liquid dropout data for Fluids 1-4 in [Table 3](#).

Fluid 1 at 405.4 K		Fluid 2 at 423.7 K		Fluid 3 at 416.2 K		Fluid 4 at 403.2 K	
Pressure bar	CVD Liquid Volume% ^{*1)}	Pressure bar	CVD Liquid Volume% ^{*1)}	Pressure bar	CME Liquid Volume% ^{*1)}	Pressure bar	CVD Liquid Volume% ^{*1)}
304.4	0	381.5	0.00	447.8	0.00	365.8	0.00
263.0	2.9	338.9	3.10	434.2	1.55	332.0	0.40
221.6	6.29	290.6	6.90	424.6	2.97	283.7	1.00
180.3	8.05	242.3	9.90	411.0	4.58	235.5	1.70
138.9	8.47	194.1	11.30	395.6	6.69	187.2	2.70
97.5	8.09	145.8	11.10	371.4	9.46	138.2	3.10

Fluid 1 at 405.4 K		Fluid 2 at 423.7 K		Fluid 3 at 416.2 K		Fluid 4 at 403.2 K	
Pressure bar	CVD Liquid Volume% ^{*1)}	Pressure bar	CVD Liquid Volume% ^{*1)}	Pressure bar	CME Liquid Volume% ^{*1)}	Pressure bar	CVD Liquid Volume% ^{*1)}
53.4	7.21	97.8	10.50	354.9	11.29	90.6	3.05
		49.3	9.60	326.9	14.06	49.3	2.90
				298.8	16.07		
				252.4	18.25		
				204.1	19.28		
				155.7	19.21		
				133.5	19.08		

^{*1)}Volume% of saturation point volume.

Table 5—Optimum equation of state parameters for the C₇₊ pseudo-components of Fluids 1-3 in Table 3 for use with the volume corrected SRK equation [2,12]. When defined components are considered, non-zero binary interaction parameters of 0.08 and 0.10 are used for N₂-C₇₊ and CO₂-C₇₊, respectively.

Fluid 1						
Cn Fractions	Mol%	Weight%	T _c K	P _c bar	Acentric Factor	Volume Correction cm ³ /mol
C ₇	20.202	13.755	551.8	35.98	0.468	-10.3
C ₈	19.596	14.871	564.7	31.90	0.500	-2.5
C ₉	15.354	13.176	581.0	28.17	0.540	5.3
C ₁₀	11.111	10.559	595.6	25.37	0.576	14.2
C ₁₁	7.677	8.003	609.8	23.11	0.612	23.4
C ₁₂	5.657	6.459	624.8	21.19	0.650	32.9
C ₁₃ -C ₁₅	10.707	14.276	653.4	18.41	0.724	51.2
C ₁₆ -C ₂₀	6.755	11.611	706.5	14.88	0.859	87.7
C ₂₁ -C ₂₅	1.922	4.259	769.0	12.17	1.013	140.0
C ₂₆ -C ₃₀	0.667	1.806	827.4	11.40	1.142	146.7
C ₃₁ -C ₃₅	0.231	0.742	883.9	11.41	1.246	120.9
C ₃₆ -C ₈₀	0.122	0.485	969.6	11.64	1.336	75.3

Fluid 2						
Cn Fractions	Mol%	Weight%	T _c K	P _c bar	Acentric Factor	Volume Correction cm ³ /mol
C ₇	16.795	9.404	537.8	33.23	0.457	9.1
C ₈	16.816	10.682	555.3	30.84	0.493	10.7
C ₉	12.539	9.069	573.0	27.21	0.534	16.4
C ₁₀	9.043	7.304	589.5	25.68	0.574	16.9
C ₁₁	6.013	5.660	612.0	22.40	0.634	22.9
C ₁₂	5.877	5.782	619.3	22.14	0.653	21.3
C ₁₃ -C ₁₅	12.992	15.064	647.1	20.62	0.731	17.0
C ₁₆ -C ₂₀	11.116	16.434	690.5	17.93	0.863	10.3
C ₂₁ -C ₂₅	4.371	8.344	740.7	16.15	1.017	-13.0
C ₂₆ -C ₃₀	2.203	5.136	785.3	15.16	1.145	-44.6

Fluid 2						
Cn Fractions	Mol%	Weight%	T _c K	P _c bar	Acentric Factor	Volume Correction cm ³ /mol
C ₃₁ -C ₃₅	1.110	3.062	826.9	14.55	1.248	-82.5
C ₃₆ -C ₈₀	1.126	4.060	909.6	13.95	1.328	-165.8
Fluid 3						
Cn Fractions	Mol%	Weight%	T _c K	P _c bar	Acentric Factor	Volume Correction cm ³ /mol
C ₇	18.427	10.019	561.4	34.83	0.454	10.5
C ₈	18.445	11.435	578.0	33.60	0.492	4.8
C ₉	10.800	7.641	595.0	33.47	0.534	-6.8
C ₁₀	8.445	6.839	615.1	23.27	0.582	38.5
C ₁₁	5.832	5.210	629.0	20.71	0.621	52.0
C ₁₂	4.568	4.462	641.3	20.58	0.658	42.1
C ₁₃ -C ₁₅	13.300	15.015	661.1	22.99	0.727	-3.9
C ₁₆ -C ₂₀	10.473	15.317	700.2	19.85	0.867	-19.0
C ₂₁ -C ₂₅	3.942	7.400	738.4	19.14	1.019	-72.1
C ₂₆ -C ₃₀	2.345	5.374	770.6	18.41	1.147	-124.4
C ₃₁ -C ₃₅	1.395	3.779	798.7	17.47	1.249	-172.1
C ₃₆ -C ₈₀	2.028	7.510	858.3	16.35	1.314	-298.0

Table 6—Equation of state parameters for defined components [13].

Component	Critical Properties			Non-zero binary interaction parameters		
	T _c K	P _c bar	Acentric Factor	N ₂	CO ₂	H ₂ S
N ₂	126.2	33.94	0.040			
CO ₂	304.2	73.76	0.225	-0.0315		
H ₂ S	373.2	89.37	0.100	0.1696	0.0989	
C ₁	190.6	46.00	0.008	0.0278	0.1200	0.0800
C ₂	305.4	48.84	0.098	0.0407	0.1200	0.0852
C ₃	369.8	42.46	0.152	0.0763	0.1200	0.0885
iC ₄	408.1	36.48	0.176	0.0944	0.1200	0.0511
nC ₄	425.2	38.00	0.193	0.0700	0.1200	0.0600
iC ₅	460.4	33.84	0.227	0.0867	0.1200	0.0600
nC ₅	469.6	33.74	0.251	0.0878	0.1200	0.0689
C ₆	507.4	29.69	0.296	0.0800	0.1200	0.0500

All components lighter than C₇ were removed from the characterized Fluids 1-3 leaving three compositions consisting exclusively of C₇₊ components. Figure 7 shows simulated phase envelopes for the resulting C₇₊ compositions, for which compositions and equation of state parameters are given in Table 5. The simulated critical temperature and pressure of the considered C₇₊ compositions increase with increasing

molecular weight. An analysis was carried out to decide whether this is a general trend for C₇₊ fractions of gas condensate fluids.

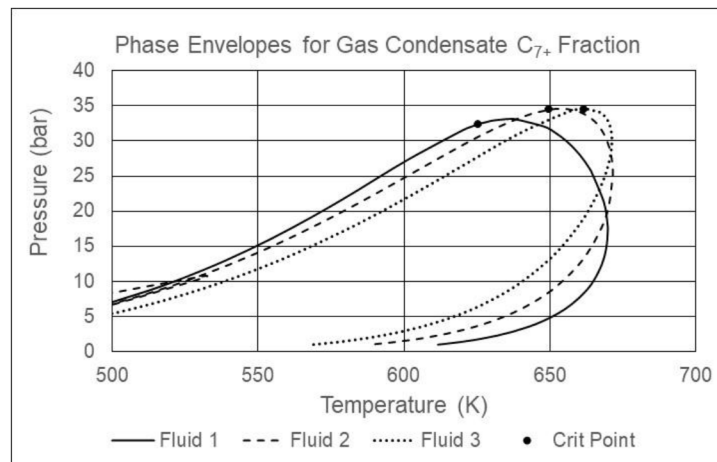


Figure 7—Simulated phase envelopes for the C₇₊ fractions of Fluid 1 (M=141.0), Fluid 2 (M=164.7) and Fluid 3 (M=167.9) in Table 3. The SRK-equation [2] has been used with the fluid descriptions in Table 5.

Using the same procedure as for the Fluids 1-3, the critical point of the C₇₊ fraction was determined for an additional 7 gas condensate mixtures. Key data for the C₇₊ fraction of the 10 gas condensate fluids is shown in Table 7. Figure 8 shows for each of the 10 fluids the critical temperature and pressures estimated for the C₇₊ fraction plotted against its average molecular weight. The observed relationship is for T_{c_C7+} and P_{c_C7+} correlated as

$$T_{c_C7+} = b_1 \times \ln(C_{7+} \text{Molecular Weight}) + b_2 \quad (10)$$

$$T_{c_C7+} = b_3 \times \ln(C_{7+} \text{Molecular Weight}) + b_4 \quad (11)$$

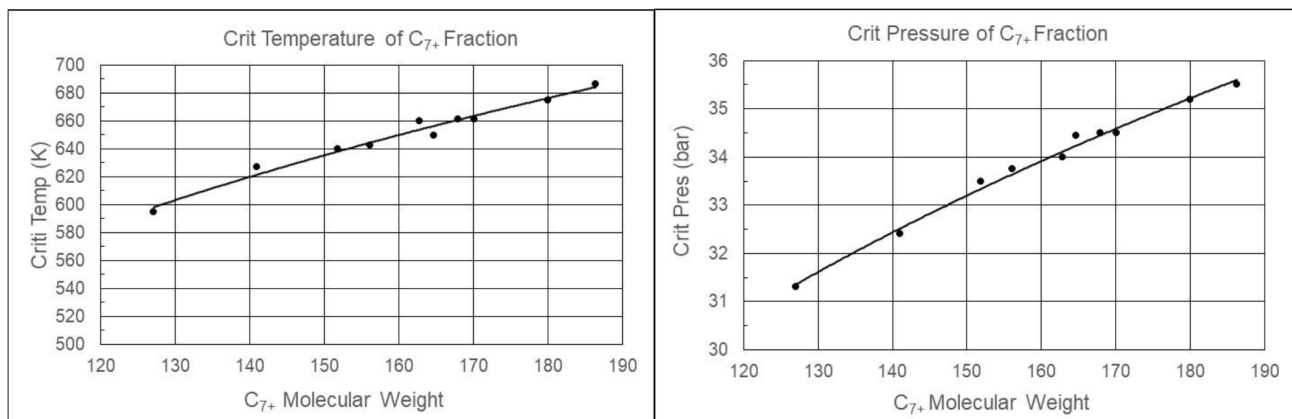


Figure 8—Critical temperature and pressure data points (•) and trend lines (—) for the C₇₊ fractions of the 10 gas condensate mixtures for which key data is shown in Table 7. The trend lines are given by Equations (10) and (11) and the values of b₁-b₄ for use with the SRK and PR equations are shown in Table 8. The shown plots are for the SRK equation.

Table 7—Key data for C₇₊ fraction of 10 gas condensate fluids. The term 4A is used to distinguish the 4th fluid from Fluid 4 in Table 3.

Fluid No.	C ₇₊ mol% of Total HC	C ₇₊ Molecular Weight	T _{res} K	P _{sat} at T _{res} bar	Reference
1	5.14	141	406.2	304.0	[14]
2	6.58	165	423.7	381.0	[4]

Fluid No.	C ₇₊ mol% of Total HC	C ₇₊ Molecular Weight	T _{res} K	P _{sat} at T _{res} bar	Reference
3	7.51	168	416.2	447.8	[15]
4A	7.27	156	405.9	359.7	[16]
5	7.36	180	403.7	523.2	—
6	10.3	170	406.5	372.6	[16]
7	3.05	127	369.8	282.0	[15]
8	3.35	152	392.1	398.0	[15]
9	5.54	163	428.2	388.0	[4]
10	10.4	186	437.2	397.2	[16]

The values of b₁-b₄ for use with the SRK and PR equations for T_{c_C7+} in K and P_{c_C7+} in bar are given in **Table 8**.

Table 8—Coefficients in Equations (10) and (11) for use with the SRK [2] and PR [3] equations to estimate T_{c_C7+} in K and P_{c_C7+} in bar for a gas condensate mixture.

Coefficient	SRK	PR
b ₁	224.92	238.08
b ₂	-491.08	-522.94
b ₃	11.300	19.994
b ₄	-24.454	-67.860

Critical Point of C₇₊ Fraction Applied in EoS Modeling

Fluid 4 was found not to have a critical point (see **Figure 5**). It is to be tested whether an estimated critical point for the C₇₊ fraction of this fluid together with the experimental saturation pressure of the reservoir fluid at the reservoir temperature is sufficient to develop a reliable EoS model for the fluid. The compositions of the reservoir fluid and its C₇₊ fraction are shown in **Table 3**. They will be handled as separate fluid compositions and a common EoS model [4] developed. That means two fluid compositions will have the same C₇₊ pseudo-components.

The critical point of the C₇₊ fraction of Fluid 4 is estimated from **Equations (10)** and **(11)**. The molecular weight of the C₇₊ fraction is shown in **Table 3**, which also shows the estimated critical point. A regression is carried out to match the saturation pressure of Fluid 4 and the estimated critical point of its C₇₊ fraction. No other PVT data is tuned to. The characterized fluids are shown in **Table 9**. The experimental (**Table 4**) and simulated CVD liquid dropout data for Fluid 4 is plotted in **Figure 9**. It is seen that the experimental liquid dropout data is matched very well despite not being tuned to.

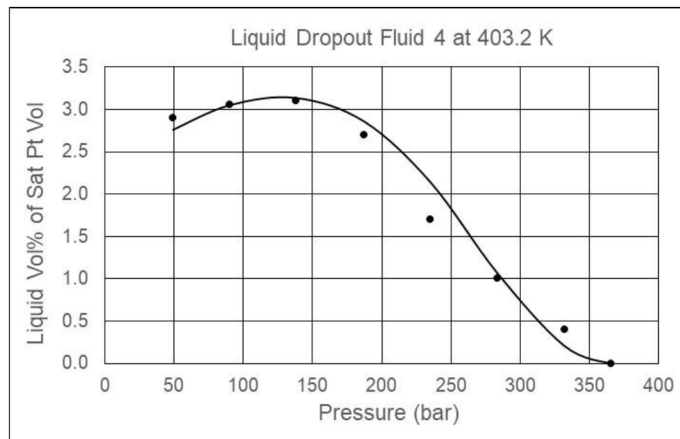


Figure 9—Experimental (●) and simulated (—) liquid dropout curve for Fluid 4 at 403.2 K using the fluid description in Table 9 and the volume corrected SRK equation. The experimental saturation pressure for Fluid 4 (Table 3) and the estimated critical point (Table 3) of its C₇₊ fraction found using Equations (10) and (11) are the only data tuned to.

Table 9—EoS model for Fluid 4 for use with the volume corrected SRK equation. The model has been developed by tuning to the experimental saturation pressure of 365.8 bar at 403.2 K for Fluid 4 and to the estimated critical point (628.5 K and 32.8 bar) of its C₇₊ fraction.

Components	Fluid 4 Mol%	C ₇₊ Fraction of Fluid 4 Mol%	T _c K	P _c bar	Acentric Factor	Volume Correction cm ³ /mol
N ₂	0.670		126.2	33.94	0.040	0.92
CO ₂	2.410		304.2	73.76	0.225	3.03
C ₁	84.480		190.6	46.00	0.008	0.63
C ₂	4.590		305.4	48.84	0.098	2.63
C ₃	2.520		369.8	42.46	0.152	5.06
iC ₄	0.440		408.1	36.48	0.176	7.29
nC ₄	0.890		425.2	38.00	0.193	7.86
iC ₅	0.310		460.4	33.84	0.227	10.93
nC ₅	0.380		469.6	33.74	0.251	12.18
C ₅	0.410		507.4	29.69	0.296	17.98
C ₇	0.550	18.966	523.9	33.78	0.453	6.08
C ₈	0.490	16.897	541.3	31.44	0.480	10.19
C ₉	0.410	14.138	561.6	27.85	0.517	17.78
C ₁₀	0.292	10.086	589.5	23.52	0.576	29.99
C ₁₁	0.233	8.051	606.0	21.87	0.612	35.45
C ₁₂	0.186	6.427	622.6	20.44	0.650	40.44
C ₁₃ -C ₁₅	0.362	12.496	652.4	18.44	0.724	47.17
C ₁₆ -C ₂₀	0.254	8.745	705.5	16.03	0.862	50.40
C ₂₁ -C ₂₅	0.082	2.835	762.3	14.66	1.012	37.98
C ₂₆ -C ₃₀	0.027	0.919	814.3	13.93	1.141	14.65
C ₃₁ -C ₃₅	0.009	0.298	862.9	13.52	1.245	-15.94
C ₃₆ -C ₈₀	0.004	0.143	932.4	13.26	1.334	-67.33

To clarify the impact of the critical point of the C₇₊ fraction on the simulated liquid dropout curve for Fluid 4, an analysis is made of the effect of tuning to a critical point of the C₇₊ composition that deviates from the optimum one found from Equations (10) and (11). The critical temperature tuned to for the C₇₊ fraction was modified by ± 20 K and the critical pressure by ± 3 bar. The resulting simulated CVD liquid dropout curves are shown in Figure 10. As can be seen from the two upper plots, the simulated critical temperature of the C₇₊ fraction has much impact on the liquid dropout curve. If the critical temperature tuned to is too high, the simulated liquid dropout will be too steep and too much liquid will dropout, while the simulation will show too little liquid drop out if the critical temperature tuned to is too low. Tuning to a too high or too low critical pressure primarily affects the high-pressure portion of the liquid dropout curve but has only a minor impact on the maximum liquid dropout.

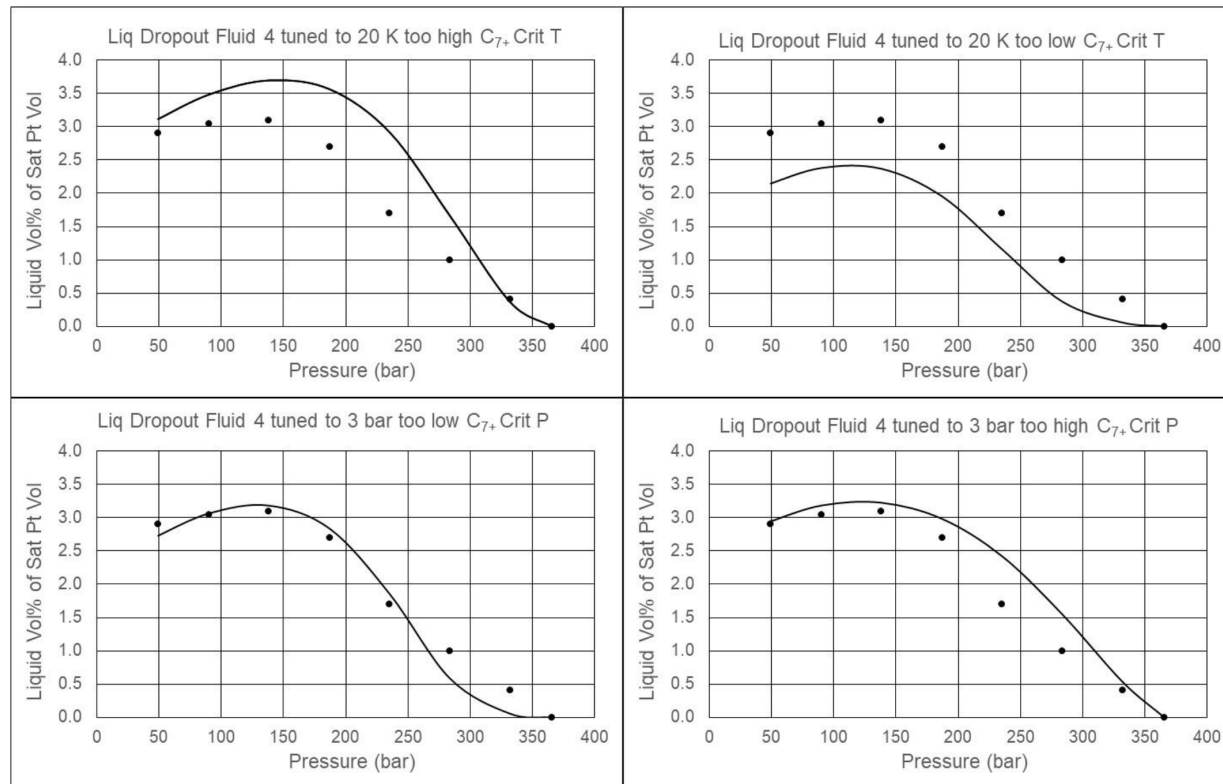


Figure 10—Impact on simulated CVD liquid dropout for Fluid 4 at 403.2 K of tuning to an incorrect critical point for the C₇₊ fraction.

Heavily Lumped Fluids

In the above examples, 12 pseudo-components were used to describe the C₇₊ fraction. If an EoS model is to be used in compositional reservoir or flow simulations, it will often be a requirement that the fluid is described using only 6-8 components to keep the calculation time low. It has been investigated for Fluid 4 whether the method that was applicable for Fluid 4 when represented as 10 defined components and 12 C₇₊ pseudo-components also can be used if the defined components are lumped down to 3 and the number of C₇₊ pseudo-components is reduced to 4 to give a fluid description counting only of 7 (pseudo-)components.

Apart from the different lumping scheme, the same procedure is used to develop the 7-component EoS model as was used for the 22-component model. The data tuned to is the measured saturation pressure of the reservoir fluid and the estimated critical point of the C₇₊ fraction, which is in this case represented using only 4 pseudo-components. The resulting characterized fluids may be seen from Table 10 and the experimental (Table 4) and simulated CVD liquid dropout data from Figure 11. Despite the heavy lumping and no other

data tuned to than a saturation pressure and an estimated critical point, a relatively good match is seen of the experimental liquid dropout curve.

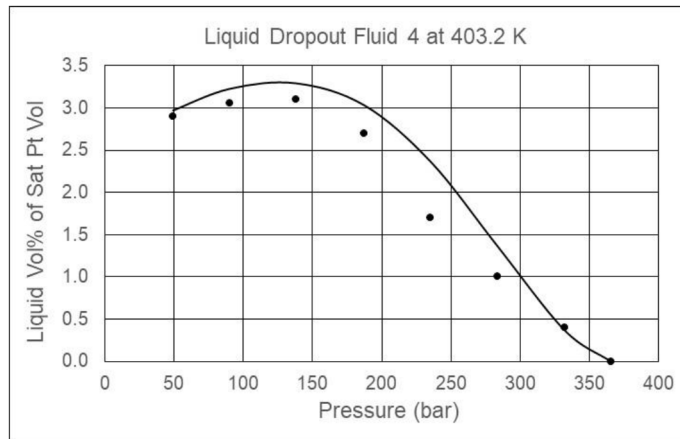


Figure 11—Experimental (●) and simulated (—) liquid dropout curve for Fluid 4 at 403.2 K using the heavily lumped fluid description in Table 10 and the volume corrected SRK equation. The experimental saturation pressure for Fluid 4 and the estimated critical point of its C₇₊ fraction (both in Table 3) found using Equations (10) and (11) are the only data tuned to.

Table 10—Heavily lumped EoS model for Fluid 4 for use with the volume corrected SRK equation [2,12]. The model has been developed by tuning to the experimental saturation pressure of 365.8 bar at 403.2 K and to the estimated critical point (628.5 K and 32.8 bar) of the C₇₊ fraction.

Components	Fluid 4 Mol%	C ₇₊ Fraction of Fluid 4 Mol%	T _c K	P _c bar	Acentric Factor	Volume Correction cm ³ /mol
N ₂ +C ₁	85.150		189.7	45.84	0.008	0.63
CO ₂ +C ₂ +C ₃	9.520		325.2	54.28	0.153	3.37
C ₄ -C ₆	2.430		452.7	34.66	0.227	10.53
C ₇ -C ₁₀	1.742	60.086	564.6	31.05	0.502	8.85
C ₁₁ -C ₂₀	1.036	35.720	659.0	22.77	0.737	-2.97
C ₂₁ -C ₃₅	0.118	4.052	764.6	18.77	1.068	-73.88
C ₃₆ -C ₈₀	0.004	0.143	873.1	17.37	1.334	-215.05

Step-by-Step EoS Modeling Procedure

Below is a step-by-step description of how to use the procedures described above to predict the critical point of either the entire reservoir fluid or its C₇₊ fraction and subsequently use the estimated critical point to develop an EoS model. In addition to the composition of the reservoir fluid, only a measured saturation pressure of the reservoir fluid at the reservoir temperature is required.

1. Generate a copy of the reservoir fluid and remove N₂, CO₂ and H₂S.
2. Calculate the mol% C₇₊ in the fluid from 1.
3. If the C₇₊ mol% is below 10, go to 7.
4. Estimate the critical point of the fluid from 1. using Equations (8) and (9) and the coefficients in Table 2 for the equation of state to be used (SRK or PR).
5. Generate a common EoS model for the reservoir fluid and the fluid from 1. Tune to the measured saturation pressure for the reservoir fluid and to the estimated critical temperature and pressure of the fluid from 1. If more PVT data is available for the reservoir fluid, that data may also be tuned to.
6. Go to 10.

7. Remove C₁-C₆ from the fluid in 1, leaving only the C₇₊ fraction.
8. Estimate the critical point of the fluid (C₇₊ fraction) from 7. using Equations (10) and (11) and the coefficients in Table 8 for the equation of state to be used (SRK or PR).
9. Generate a common EoS model for the reservoir fluid and the fluid from 7. Tune to the measured saturation pressure for the reservoir fluid and to the estimated critical temperature and pressure of the fluid from 7. If more PVT data is available for the reservoir fluid, that data may also be tuned to.
10. Use the EoS model developed for the reservoir fluid. It is applicable at both reservoir and process conditions.

Discussion

The findings about the influence of the location of the critical point on the phase behavior of a reservoir fluid in the entire gas and liquid region can be used in various ways. An obvious application would be to limit the extent of experimental PVT studies to only cover a measured saturation pressure at the reservoir temperature and develop the EoS model by tuning to the saturation pressure at the reservoir temperature and the estimated critical point of either the reservoir fluid stripped of inorganics or its C₇₊ fraction. An alternative approach could be to redesign the classical PVT experiments to enable the critical point of either the entire reservoir fluid or its C₇₊ fraction to be determined. For reservoir oils, the critical point can be determined from swelling data [11,14]. The same technique could in principle be used on the liquid from a flash of a gas condensate sample to standard conditions, but this would require enough liquid to perform a swelling experiment. However, the PVT studies that are carried out per standard by commercial PVT laboratories are so well established that they are unlikely to be changed. With a standard PVT report available, the critical point of either the total reservoir fluid for oil mixtures or of the C₇₊ fraction for gas condensates can instead be used as an additional (artificial) data point (constraint) when developing an EoS model matching the experimental PVT data. This will ensure that the model is applicable not only at the temperature for which PVT studies have been carried out, but also at the conditions, the fluid will experience during production. If an EoS model already exists, the methods described in this paper can be used to check whether the model is generally applicable. For an oil mixture, the critical temperature of the fluid after removal of inorganics should agree with Equation (8) within ± 20 K, and the critical pressure with Equation (9) within ± 10 bar. For a gas condensate, the critical temperature of the C₇₊ fraction should agree with Equation (10) within ± 10 K, and the critical pressure with Equation (11) within ± 2 bar.

Conclusion

For a pure component it is a basic assumption of a cubic equation of state that the phase behavior is essentially determined by the location of the critical point. It is shown that the critical point also for a multi-component petroleum reservoir fluid exerts a strong influence on the phase behavior throughout the gas and liquid regions. If the critical point and the saturation pressure at the reservoir temperature are matched, the phase behavior of the fluid will be matched at practically all conditions of interest in oil and gas production. Correlations are presented enabling the critical point of a reservoir oil stripped of inorganics to be estimated from the molar ratio of C₇₊ to lighter components. Not all gas condensates will have a critical point, but the critical point of the C₇₊ fraction of a gas condensate can be determined from its molecular weight. The lighter components have well-defined critical properties and can subsequently be added in the correct molar amounts to get an EoS model applicable to the entire gas condensate reservoir fluid. It is shown that the procedure can be used to develop a reliable EoS model even when the only experimental data available is a reservoir fluid composition and the saturation pressure at the reservoir temperature. When more PVT data is available, the estimated critical point can be used as an artificial additional data point (constraint) when tuning to experimental PVT data. This is particularly useful when developing a heavily lumped EoS model.

List of Notation

A	Constant in Equation (1)
a_1-a_5	Coefficients in Equations (8) and (9)
B	Constant in Equation (1)
b_1-b_4	Coefficients in Equations (10) and (11)
C _n	Carbon number
CME	Constant mass expansion
CP	Critical point
CVD	Constant volume depletion
C ₇₊	Components with a normal boiling point exceeding that of nC ₆
c _{1-c₄}	Coefficients in Equation (3)
d _{1-d₅}	Coefficients in Equation (4)
EoS	Equation of state
e _{1-e₄}	Coefficients in Equation (5)
HC	Hydrocarbon
M	Molecular weight
m	Polynomial in acentric factor defined in Equations (5) and (6)
P	Pressure
PR	Peng-Robinson
SRK	Soave-Redlich-Kwong
T	Temperature
V/L	Vapor/liquid volume fraction
vdW	van der Waals
z	Mole fraction

Greek letters

ρ	Density
ω	Acentric factor

Sup and Super Indices

c	Critical
i	Component index
mix	Mixture
res	Reservoir

References

1. J.D. van der Waals, Doctoral Dissertation, Over de Continuiteit van der Gas- en Vloeistofstoestand Leiden, University, The Netherlands, 1873 (In Dutch).
2. G. Soave, Equilibrium constants from a modified Redlich-Kwong equation of state, *Chem. Eng. Sci.* **27**, 1197–1203. 1972.
3. D.-Y. Peng, and D.B. Robinson, The characterization of the heptanes and heavier fractions for the GPA Peng-Robinson Programs, GPA Research Report RR-28, 1978.
4. K.S. Pedersen, P.L. Christensen and J.A. Shaikh, Phase Behavior of Petroleum Reservoir Fluids, 3rd edition, CRC Press, 2023.

5. K.S. Pedersen, P. Thomassen and A. Fredenslund, Thermodynamics of petroleum mixtures containing heavy hydrocarbons. 1. Phase envelope calculations by use of the Soave-Redlich-Kwong equation of state, *Ind. Eng. Chem. Process Des. Dev.* **23**, 163–170, 1984.
6. K.S. Pedersen, A.L. Blilie and K.K. Meisingset, PVT simulation on petroleum reservoir fluids using measured and estimated compositional data for the plus fraction, *Ind. Eng. Chem. Res.* **31**, 1378–1384, 1992.
7. H. Sørensen, K.S. Pedersen and P.L. Christensen, Method for generating shale gas fluid compositions from depleted sample, presented at the International Gas Injection Symposium, Calgary, September 24-27, 2013.
8. R.R. Boesen, S. Lekumjorn. C. Agger and H. Sørensen, Chemical Reaction Equilibrium Theory - A Novel Approach to Estimate Shale Reservoir Fluid Compositions, SPE-213222-MS, presented at the *Middle East Oil, Gas and Geosciences Show*. February 19-21, 2023.
9. K.S. Pedersen, J. Milter and H. Sørensen, Cubic equations of state applied to HT/HP and highly aromatic fluids, *SPE J.* **9**, 186–192, 2004.
10. P.L. Christensen, Regression to experimental PVT data, *J. Can Petroleum Technol.* **38**, 1–9, 1999.
11. K.S. Pedersen, J.A. Shaikh and P.L. Christensen, Importance of critical point for the phase behavior of a reservoir fluid, *Fluid Phase Equilibria* **573**, 2023.
12. A. Peneloux, E. Rauzy and R.A. Fréze, A consistent correction for Redlich-Kwong-Soave volumes, *Fluid Phase Equilibria* **8**, 7–23, 1982.
13. H.R. Knapp, R. Döring, L. Oellrich, U. Plöcker and J.M. Prausnitz, Vapor-liquid equilibria for mixtures of low boiling substances, *Chem. Data Ser. Vol. VI*, DECHEMA, 1982.
14. A. Kumar, M.E. Gohary, K.S. Pedersen, and J. Azeem, Gas injection as an enhanced recovery technique for gas condensates. A comparison of three injection gases, SPE 177778-MS, presented Abu Dhabi International Petroleum Exhibition and Conference in Abu Dhabi, UAE, 9–12 November 2015.
15. K.S. Pedersen, P. Thomassen and A. Fredenslund, Characterization of Gas Condensate Mixtures, *Advances in Thermodynamics* **1**, 137–152, 1989.
16. A. Takeshi, F. Tetsuro, S. Leekumjorn, J.A. Shaikh, K.S. Pedersen, A. Alobeidli and K. Mogensen, A new technique for common EoS model development for multiple reservoir fluids with gas injection, SPE-202923-MS, The Abu Dhabi International Petroleum Exhibition & Conference (ADIPEC), November 9-12, 2020.